Controlled Intracellular Release of Camptothecin by Glutathione-Driven Mechanism

P. Botella*, C. Muniesa*, V. Vicente**, K. Fabregat* and A. Cabrera-García*

*Instituto de Tecnología Química (UPV-CSIC), Av. Los Naranjos s/n, 46022 Valencia, Spain, pbotella@itq.upv.es

** Universidad de Investigación de Tecnología Experimental YACHAY, Imbabura, Ecuador

ABSTRACT

Novel nanomedicines for the intracellular controlled release of camptothecin (CPT) are presented. A new synthetic strategy has been implemented by direct coupling of as synthesized (pyridin-2-yldisulfanyl)alkyl carbonate derivatives of CPT with thiol groups of silica hybrid nanoparticles containing a non-porous core and a mesoporous shell. Upon reaction with thiols in physiological conditions, disulfide bridge cleavage occurs, releasing the naked drug after an intramolecular cyclization mechanism. Additional incorporation of rhodamine B (RhB) into particle core facilitates imaging at the subcellular level for the monitoring of uptake and delivery. This novel CPT-containing nanoparticulated system combines therapeutic activity and imaging, imposing controlled intracellular release of the active principle under the reducing activity of GSH.

Keywords: cancer therapy, drug delivery, camptothecin, hybrid materials, redox-sensitive

1 INTRODUCTION

Nanomedicine rating in the pharmaceutical market is rising in the last years due to their advantages over single therapeutic molecules like plasma stability, lower toxicity and controlled release [1-3]. The incorporation of a drug to a nanoparticle can be carried out by simple click-chemistry reactions that provide good stability to the conjugate [4,5]. Unfortunately, direct coupling of antitumor drugs to nanoparticles is circumvented by the reduced therapeutic activity of the structure-modified derivatives [6]. It is desirable to develop covalent linking models that allow for the controllable release of the free drug after cell entry [7]. To address this target, recently we have developed a novel CPT nanoplatform based in a mercapto-functionalized silica hybrid containing a non porous core and a mesoporous shell (SiO_2@MSN). (Pyridin-2-yldisulfanyl) ethyl carbonate derivative of CPT has been synthesized and attached over the pores of the thiol modified inorganic nanoparticles by disulfide bridge (SiO_2@MSN-CPT). This bond is sensitive to intracellular reducing compounds as glutathione (GSH), releasing free CPT after an intramolecular cyclization [8]. Here, we extend the material study to other CPT prodrugs and present the *in vitro* evaluation of these nanomedicines in HeLa cancer cell line, stating their cytotoxic activity as well as the intracellular release mechanism.

2 EXPERIMENTAL

All reagents and solvents were purchased from Sigma-Aldrich except HPLC solvents (HPLC grade from Scharlab or LC/MS grade Optima from Fisher). HeLa cells were originally obtained from the American Type Culture Collection (Rockville, MD) maintained in RPMI media supplemented with 10% fetal bovine serum (FBS, from Lonza, Verviers, Belgium) at 37 ºC under a humidified atmosphere of 95% air and 5-10% CO_2.

2.1 Preparation of CPT prodrugs

(Pyridin-2-yldisulfanyl)alkyl carbonate derivatives of CPT (alkyl=ethyl, propyl, buthyl) were synthesized following procedures reported earlier (compounds **1a-c)** [8]. The purity of all obtained molecules was determined by RP-HPLC and the chemical structure was confirmed by ^{1}H NMR, ^{13}C NMR and Q-TOF MS analysis.

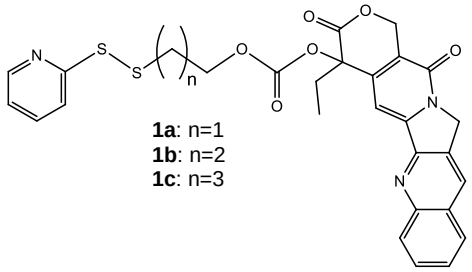

Figure 1: Redox sensitive CPT prodrugs synthesized in this work.

2.2 Preparation of CPT nanomedicines

50 nm average diameter fluorescent amorphous silica cores were synthesized as reported elsewhere [8,9]. These cores were suspended in ultra-pure water (3 mL) and mixed with a solution of CTAB (100 mL, 8 mM) and NaOH (1 mL, 100 mm). Then, a TEOS solution in ethanol (0.3 mL, 20% v/v) was added three times every 30 min. The mixture was allowed to stir for 2 h at 60 ºC and afterwards a solid was separated by centrifugation (12500 g, 15 min) and washed with ethanol. Remaining in pores CTAB was extracted for 20 hours at 80 ºC with 20 mL of a mixture

ethanol:n-heptane (48:52) containing HCl 0.15 M. The solid was again centrifuged (12500 g, 15 min), washed with ethanol and freeze-dried. Core-shell nanoparticles (SiO_2@MSN) were dried under vacuum at 75 ºC for 6 hours. Then, anhydrous toluene (0.5 mL) and (3-mercaptopropyl)trimethoxysilane (0.32 mL) was added, and the mixture was stirred at 120 ºC for 16h. Hybrid nanoparticles (SiO_2@MSN-SH) were filtered and washed with toluene and methanol. 100 mg of these particles were suspended in DTT solution (10 mL, 100 mM) and stirred for 30 minutes. Then, the suspension was centrifuged (12500 g, 15 min) and the solid obtained was washed with methanol. Afterwards, a solution of the prodrug, **1a**, **1b** or **1c** (3.3 mL in DMSO, 10 mg mL^{-1}), and methanol (16 mL) was added, and the mixture was stirred for 16 h. Then, the suspension was centrifuged (12500 g, 15 min) and the obtained solid (SiO_2@MSN-CPT) was washed with methanol repeatedly until no rest of prodrug or CPT was detected by UV-Vis (A_{368}), and was freeze-dried. Nanomedicines were characterized by powder XRD, nitrogen gas adsorption isotherms (BET and KJS methods), TEM, diffuse light scattering (DLS), Z-potential and diffuse-reflectance UV-Vis.

2.3 GSH-triggered release of CPT

The release of CPT from SiO_2@MSN-CPT samples (Figure 2) was monitored by placing 5 mg of material in a vial with 1 mL of PBS solution. The tube was vigorously shaken using a vortex for 30 seconds. Then the suspension was placed in a Thermomixer® at 37º C and 1350 rpm. After 2 hours, 3.1 mg of GSH was added to the solution to reach 10 mM concentration of reducing agent. At the corresponding time the sample was centrifuged (12500 g, 15 min) and the supernatant was freeze-dried and further dissolved with 950 μL of methanol and 50 μL of HCl 1 M solution. This sample was analyzed by RP-HPLC and ESI-MS. Triplicate samples were run for every experiment.

2.4 *In vitro* study

HeLa cells (4000 cells/well, 96-well plates) were treated with CPT loaded nanocarriers or CPT (in DMSO), with final doses ranging from 0.0025 to 2.5 μg mL^{-1} (in CPT equivalents) during 72 hours. At the end of the incubation period, MTT solution in PBS was added at a final concentration of 0.2 mg mL^{-1} to the wells and 4 h later formazan crystals were dissolved in DMSO and spectrophotometrically measured at 550 nm. Half maximal inhibitory concentration (IC_{50}) data were evaluated by variable slope curve-fitting using Prism 5.0 software (GraphPad, San Diego, CA). Three independent experiments were performed for every sample, and each experiment was carried out with five points per concentration.

Cell internalization of nanomedicines and intracellular CPT release was monitored by confocal laser scanning microscopy (CLSM), using excitation peaks at 488/561 nm and emission at 522/585 nm for LysoTracker® and RhB, respectively. Images were acquired at 60x magnification at every μm, with an optical resolution of about 800 nm.

In order to demonstrated the active role of GSH in CPT release, we performed MTT experiments after GSH inhibition. For this purpose, HeLa cells (4000 cells/well, 96-well plates) were incubated for 24 h with L-buthionine sulfoximine (BSO, 0.1 mM) or chloroquine (CLQ, 0.15 mM). After incubation, growth medium was exchanged and cells with fresh medium were treated with SiO_2@MSN-CPT-1 or CPT (in DMSO), with final doses ranging from 0.0025 to 2.5 μg mL^{-1} (in CPT equivalents) during 72 hours. At the end of the incubation period IC_{50} calculation survival data were evaluated as described above. Three independent experiments were performed for every sample, and each experiment was carried out with five points per concentration.

3 RESULTS AND DISCUSSION

Particles with a diameter of around 50-60 nm, a non-porous core and a wormhole-like mesoporous shell were synthesized. Diffuse reflectance UV-vis spectroscopy of SiO_2@MSN-CPT samples showed broad absorption bands at 368 nm (CPT) and 560 nm (RhB, Fig. 2b). The loading of these molecules was 4.5-4.7 % of the dye (as determined by elemental analysis) and 0.9-3.5 % of the drug (as measured by RP-HPLC after release, see Table 1).

The sensitivity to reducing agents of the nanomedicines was assayed by measuring (RP-HPLC and ESI-MS) their

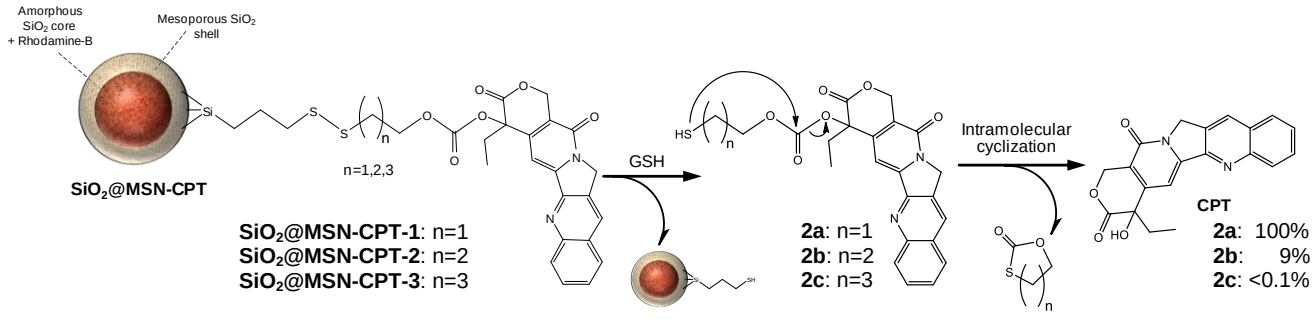

Figure 2: Design of the novel CPT nanomedicines and the release mechanism driven by reducing compounds.

decomposition when incubated 6 hours at 37 ºC in phosphate buffered saline (PBS, 1x, pH 7.4) with 10 mM GSH. Disulfide cleavage took place quickly in all cases (Figure 2). However, the desired following intramolecular cyclization and cleavage of the neighboring carbonate bond of **2a-c** to yield free CPT, CO_2 and the corresponding thiolactone only happened quantitatively for 2**a** compound. Conversely, carbonate **2b** released only 5% CPT and **2c** showed only traces of the therapeutic molecule. This pattern of stability of the carbonate derivative correlates to the increasing distance between the carbonyl group and the proximal sulfur atom, and agrees strongly with the behavior observed for similar disulfide conjugates of luciferin [10].

MTT cytotoxicity experiments were conducted by incubating during 72 h HeLa cancer cells with the different nanomedicines (0.0025 to 2.5 μg mL^{-1} in CPT equivalents) and IC_{50} values were determined (Table 1). SiO_2@MSN-CPT-1 sample and free CPT presented very similar value of cell survival. However, nanomedicines with longer lateral chain (n=2,3) showed one order higher IC_{50} values. Actually, these samples release mostly the reduced prodrugs (**2b,c** compounds), which are much less active than CPT. **2b,c** molecules might release CPT by carbonate hydrolysis but, in our experimental conditions, this is a slower process than the intramolecular cyclization [8].

The internalized particles were visually observed by CLSM. To investigate successful cell entry and intracellular location of nanomedicines co-localization experiments were conducted by incubating HeLa cells with SiO_2@MSN-CPT-1 particles. Confocal images acquired at different heights along the Z-axis after 24 h incubation show nanoparticles co-localizing with lysosomes (Figure 3). At this incubation time, nanoparticles can also be seen outside lysosomes which means that the nanoparticles are able to shift into cytosol. Here, recent research points to endosomal escape as a bottle-neck for stimuli-responsive models based on redox-driven intracellular disulfide cleavage [11]. However, the negative surface charge of SiO_2@MSN-CPT-1 (ζ=-17.0±6.6 mV) can promote the escape of nanoparticles from endo-lysosomal compartments and enter the cytosol to release their cargo [12].

Many authors point out the role of GSH for disulfide cleavage and cytosolic release [7,13-16]. Nevertheless, the endosomal/lysosomal reducing activity mediated by protein disulfide isomeraseI [17] or endosomal reductase [18], could also bring an early download of the

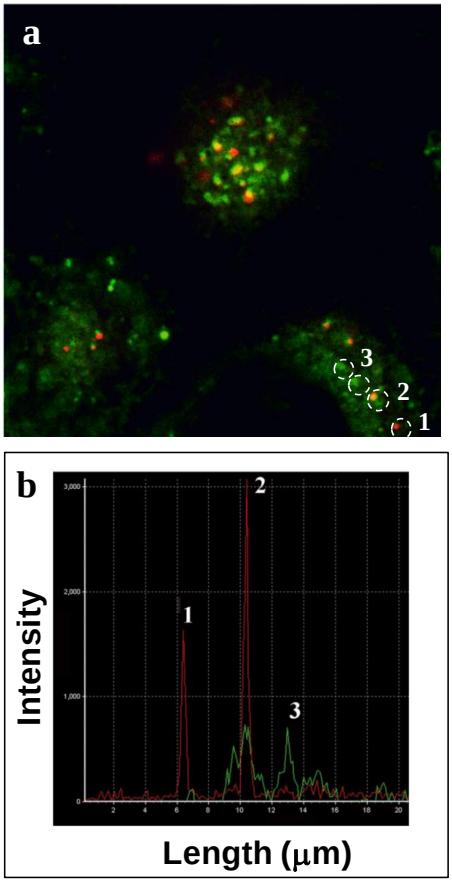

Figure 3: Co-localization studies of SiO_2@MSN-CPT-1 in HeLa cells. Confocal images of the same Z plane obtained for LysoTracker® and RhB are merged in (a) showing nanoparticles found in cytosol (1), nanoparticles co-localizing with lysosomes (2) and lysosomes without nanoparticles (3). Signal intensity for all these items is depicted in (b).

the therapeutic molecule. In addition, it must be taken into account that carbonate bonds could also be cleaved by unspecific cytosolic carboxylases [19]. Therefore, to provide further evidence of GSH role in CPT release mechanism the cytotoxic activity of SiO_2@MSN-CPT-1 was studied by MTT assay in the presence of GSH synthesis inhibitors like BSO and CLQ [20,21]. BSO or CLQ was added to a concentration of 0.1 or 0.15 mM, respectively, 24 h before nanomedicine incorporation to deplete GSH levels in HeLa cells. In bothcases, it was

Sample	**Prodrug**	**CPT content (%, wt/wt)**	**Area BET (m^2/g)**	**Inhibitor**	**IC_{50}**
CPT	---	---	---	none	0.0064±0.0007
SiO_2@MSN-CPT-1	**1a**	3.5	114.9	none	0.0067±0.0005
SiO_2@MSN-CPT-2	**1b**	2.0	164.5	none	0.0510±0.0002
SiO_2@MSN-CPT-3	**1c**	0.9	537.9	none	0.0462±0.0006
SiO_2@MSN-CPT-1	**1a**	3.5	114.9	BSO 0.1 mM	0.0211±0.0013
SiO_2@MSN-CPT-1	**1a**	3.5	114.9	CLQ + 0.15 mM	0.0265±0.0027

Table 1: IC_{50} values (mean ± SEM, in μg mL^{-1}) for free CPT and SiO_2@MSN-CPT nanomedicines in HeLa cells (n=3).

found that GSH synthesis provokes a very powerful reduction effect of nanomedicine cytotoxicity, with IC_{50} value becoming three-four times the experiment with no inhibitor. These findings support the role of GSH in the activation of the intramolecular cyclization that commands drug release, regardless of other possible mechanism that could also be involved in the CPT intracellular discharge.

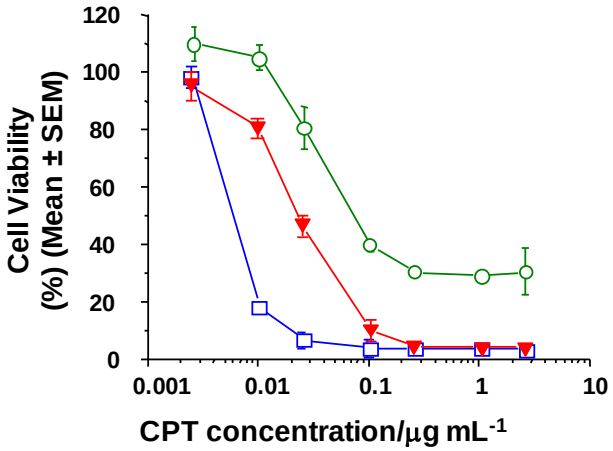

Figure 4: Effect of GSH depletion level by inhibitors like BSO or CLQ, in the cytotoxic activity of SiO_2@MSN-CPT-1. Legend: (□) SiO_2@MSN-CPT-1; (▼) SiO_2@MSN-CPT-1+BSO 0.1 mM; (○)SiO_2@MSN-CPT-1+CLQ 0.15 mM. Concentration corresponds to CPT equivalents.

4 CONCLUSION

Controlled intracellular release of CPT may be achieved through a GSH-driven mechanism. For this purpose, novel core-shell nanomedicines combining therapeutic activity and imaging at the subcellular level have been developed, based in an external covalent coupling model with a cleavable disulfide linker able to release CPT by means of an intramolecular cyclization mechanism and using RhB as internal fluorophore. A new synthetic strategy has been implemented by direct incorporation of CPT prodrugs on the nanocarrier. The length of the linking chain of CPT to the nanocarrier is crucial in drug release and cytotoxicity, and only short linkers allow for controlled and complete discharge of the drug under cytosolic GSH reducing activity. The valuable stability provided in physiological medium points to an optimized delivery system able to surpass extracellular and intracellular barriers in order to monitor a fine control over releasable species.

ACKNOWLEDGMENT

The authors are thankful for financial support to the Spanish Ministry of Economy and Competiveness (projects SEV-2012-0267, MAT2012-39290-C02-02 and IPT-2012-0574-300000). We kindly appreciate the technical support of the Electronic Microscopy Service of UPV.

REFERENCES

[1] T. Elbayouni and V. Torchilin, "Nanomedicine in Health and Disease", Science Publishers Inc., Enfield, NH, 2011.
[2] Y. Cao and R. Langer, Sci. Transl. Med. 2, 15ps3, 2010.
[3] I. Ojima, Pure Appl. Chem. 83, 1685, 2011.
[4] P. Botella, I. Abasolo, Y. Fernández, C. Muniesa, S. Miranda, M. Quesada, J. Ruiz, S. Schwartz Jr. and A. Corma, J. Controlled Release 156, 246, 2011.
[5] L. Tang, T. M. Fan, L. B. Borst and J. Cheng, ACS Nano 6, 3954, 2012.
[6] M. L. Rothenberg, Ann. Oncol. 8, 837, 1997.
[7] J. Chen, S. Chen, X. Zhao, L.V. Kuznesova, S.S. Wong and I. Ojima, J. Am. Chem. Soc. 130, 16778, 2008.
[8] C. Muniesa, V. Vicente, M. Quesada, S. Saez-atienzar, J. R. Blesa, I. Abasolo, Y. Fernandez and P. Botella, RSC Adv. 3, 15121, 2013.
[9] D. Ma, A. J. Kell, S. Tan, Z. J. Jakubek and B. Simard, J. Phys. Chem. C 113, 15974, 2009.
[10] L. R. Jones, E. A. Goun, R. Shinde, J. B. Rothbard, C. H. Contag and P. A. Wender, J. Am. Chem. Soc. 128, 6526, 2006.
[11] A. M. Sauer, A. Schlossbauer, N. Ruthardt, V. Cauda, T. Bein and C. Bräuchle, Nano Lett. 10, 3684, 2010.
[12] I. Slowing, B. G. Trewyn and V. S.-Y. Lin, J. Am. Chem. Soc. 128, 14792, 2006.
[13] R. Cheng, F. Feng, F. Meng, C. Deng, J. Feijen and Z. Zhong, J. Controlled Release 152, 2, 2011.
[14] G. Saito, J. A. Swanson and K.-D. Lee, Adv. Drug Deliver. Rev. 55, 199, 2003.
[15] M. H. Lee, J. Y. Kim, J. H. Han, S. Bhuniya, J. L. Sessler, C. Kang and J. S. Kim, J. Am. Chem. Soc. 134, 1316, 2012.
[16] H. Kim, S. Kim, C. Park, H. Lee, H. J. Park and C. Kim, Adv. Mater. 22, 4280, 2010.
[17] Y.-C Wang, F. Wang, T.-M. Sun and J. Wang, Bioconjugate Chem. 22, 1939, 2011.
[18] J. Yang, H. Chen, I. R. Vlahov, J.-X. Cheng and P. S. Low, Proc. Natl. Acad. Sci. USA 103, 13872, 2006.
[19] W. A. Henne, D. D. Doorneweerd, A. R. Hilgenbrink, S. A. Kularatne and P. S. Low, Bioorg. Med. Chem. Lett. 16, 5350, 2006.
[20] G. K. Balendiran, R. Dabur and D. Fraser, Cell Biochem. Funct. 22, 343, 2004.
[21] H. Ginsburg, O. Famin, J. Zhang and M. Krugliak, Biochem. Pharmacol. 56, 1305, 1998.